frontiers | Frontiers in Earth Science

TYPE Original Research
PUBLISHED 12 January 2023
DOI 10.3389/feart.2022.1062738

OPEN ACCESS

EDITED BY
Fangtian Wang,
China University of Mining and Technology, China

REVIEWED BY
Bangyou Jiang,
Shandong University of Science and Technology, China
Xuejie Deng,
China University of Mining and Technology Beijing, China

*CORRESPONDENCE
Leiming Zhang,
zhangleiming@stu.xust.edu.cn

SPECIALTY SECTION
This article was submitted to Structural Geology and Tectonics, a section of the journal Frontiers in Earth Science

RECEIVED 06 October 2022
ACCEPTED 31 October 2022
PUBLISHED 12 January 2023

CITATION
Zhang L, Lai X and Bai R (2023), Study of the response characteristics of the water–force coupling action of hard coal bodies in steeply inclined coal seams.
Front. Earth Sci. 10:1062738.
doi: 10.3389/feart.2022.1062738

Study of the response characteristics of the water–force coupling action of hard coal bodies in steeply inclined coal seams

Leiming Zhang[1,2]*, Xingping Lai[1,2] and Rui Bai[3]

[1]School of Energy Engineering, Xi'an University of Science and Technology, Xi'an, China, [2]Key Laboratory of Western Mines and Hazards Prevention, Ministry of Education of China, Xi'an, China, [3]National Energy Group Ningxia Coal Industry Co., Ltd. Qingshuiying Coal Mine, Lingwu, China

Study of the pre-blast weakening of hard-top coal water injection is especially important to solve problems related to the low recovery rate of coal resources and frequent dynamic disasters due to the low degree of fragmentation of hard-top coal during high-stage fully mechanized top-coal caving in steeply inclined coal seams. With the application of rock mechanical tests and numerical simulations, this study carries out mechanical property testing on natural and water-saturated coal samples, investigates the effect of moisture on coal sample mechanical properties in meso-scale, and quantifies the degradation of coal samples under moisture due to mollification. It also reveals the interaction between water and acoustic emission signals based on the statistics of acoustic emission count and energy. A numerical model is established to analyze coal sample internal stress distribution features before and after water injection in macro-scale. Moreover, the detailed mitigating measures for top-coal water injection for engineering practice are designed. The results demonstrate that the mechanical properties of coal samples are significantly affected by moisture-induced degradation. The failure and collapse degrees of water-saturated samples are generally larger than those of natural samples. When the water content is higher, the acoustic emission count and energy of the coal sample are smaller—presenting a negative correlation. The internal stress of coal samples before and after water injection differs significantly. When subjected to water, the top-coal stress releases and transfers, and the peak value is significantly reduced. This study has verified in macro- and meso-scales that top coal can be fully weakened under water–force coupling. The findings of this study are of practical significance for safe and efficient mining and provide a reference for presplit weakening of hard-top coal during horizontal sublevel fully mechanized top-coal caving in steeply inclined coal seams.

KEYWORDS

top-coal presplit, fully mechanized caving mining, coupling effect, water-injection weakening, steeply inclined coal seams

Introduction

Coal will remain the main integral energy in China for a long time. The Urumqi mining area in the west of China is rich in coal resources and is a strategic energy reserve area (Qian, et al., 2018; Zhang, et al., 2020; Lai, et al., 2022). However, the Urumqi mining area typically has 45°–87° steeply inclined coal seams, and consequently the mining process and technology of this steep lamination are very complex. High-stage horizontal sublevel fully mechanized caving mining is mostly adopted in current practice (Shi and Gao, 2003; Wang, 2018; Lai, et al., 2020; Wu, et al., 2020). Along with the mining process, problems such as the low degree of hard-top coal breakage and difficulty in releasing from the coal outlet are increasingly becoming prominent. This results in low top-coal recovery rate and the collapse of top coal in the goaf, which can easily induce a dynamic disaster. This seriously restricts the safe and efficient mining of these mines. Therefore, an investigation of advanced pre-crack weakening technology for the hard-top coal of steeply inclined coal seams is urgently required.

In recent years, many scholars at home and abroad have carried out a lot of basic theoretical research on the pretreatment and weakening technology of the hard-top coal of steeply inclined coal seams. In terms of the special occurrence features of steeply inclined coal seams, Ju et al. (2006) studied the appearance law and dynamic pressure influence characteristics of steeply inclined coal seams in Huating Coal Mine. Dai et al. (2006) applied the similarity simulation method to reveal the characteristics and laws of strata and surface movement induced by deep mining of steeply inclined coal seams. Li (2018) proposed a technical scheme and implementation approach of fully mechanized caving mining in a hard extra-thick seam in the Yushen Mining Area. Wu and Shi (1990) discussed the release rule and mine pressure development rule of top coal that is broken by the steep seam using a simulation test rack. Lai et al. (2009) investigated a roof collapse during the mining of steeply inclined coal seams in Weihuliang Coal Mine and effectively prevented the occurrence of a dynamic disaster. Meanwhile, pre-cracking technology of hard-top coal in a fully mechanized caving face has also been investigated. Xie et al. (1999) and Wang et al. (2000) discussed a pre-loosening blasting crushing technical scheme in a hard-thick seam and proved its good performance in application. Deng et al. (2004) investigated the mechanism of fracture development and propagation in coal samples during the water–force coupling fracturing process and conducted experiments on the relationship between fracture initiation and propagation of a coal sample under water pressure and the permeability of the coal sample, revealing the mechanical mechanism of hydraulic coal breaking. Suo (2001) implemented a comprehensive weakening method of pre-water injection and deep-hole blasting in a hard-top coal workface at Honghui No.1 Mine, which effectively solved the problem of large caving blocks in the top coal. Aiming at the special conditions of a hard seam at Datong Yungang Coal Mine, Yang (2014) adopted the combined weakening measure of water injection-explosion to fully combine the respective advantages of water injection and blasting measures. A set of weakening methods and measures suitable for a fully mechanized caving hard-top coal workface have been proposed. For example, Cui et al. (2015) studied steep ultra-thick coal rock, and designed and implemented a coupling–cracking scheme for steeply inclined coal seams. Their field practice results show that, after taking the coupling–cracking measurement, the cavitability, fragmentation degree, and recovery rate of top coal were significantly improved and the frequency of dynamic disasters was significantly reduced.

These scholars have actively explored and studied mining pressure development, mining technology, and pre-crack weakening technology for steeply inclined coal seams but mainly focused on the design parameter and scheme optimization of the pre-crack weakening scheme of hard-top coal. From these studies, it can also be found that whether using single water injection weakening or water injection-blasting coupled pre-blast weakening, it is clear that water-injection treatment is a key and necessary measure in the process of pre-blast weakening. Meanwhile, the occurrence of steeply inclined coal seams is more complicated. There is no research on the pre-blast and weakening technology for the hard-top coal of steeply inclined coal seams. In particular, the weakening-damage features of water-injection weakening and the response relationship between water injection and stress need to be studied further. In view of this, the authors took the north mining area of the Wudong Coal Mine as the background. Rock mechanics test and numerical calculation were used to study the response features of steeply inclined coal seams in the water–force coupling at macro- and micro-scales. The stress distribution law of the coal sample and the strength degradation and destruction of a coal sample under moisture-induced degradation are investigated. A specific top coal water-injection weakening scheme was proposed based on the actual situation in the field to provide rational guidance for the pre-blast and weakening of hard-top coal during horizontal sublevel fully capped caving in steeply inclined coal seams with similar conditions.

Engineering background

Wudong Coal Mine is located in Midong District, Urumqi City, Xinjiang, which is located on the border of Bogda Mountain and Jungar Basin, with a mine field area of about 20 km^2. The coal seams' dip angle in the mine's north mining area is 43°–51°, which means that they are steeply inclined coal seams. Currently, 43# and 45# coal seams are mainly mined. The average thickness of the two coal seams is 28.28 m and 21.21 m, respectively, and the dip angles are both 45°. The coal seam structure is simple and contains a small amount of carbonaceous mudstone or siltstone intercalated gangue. The occurrence characteristics of coal seams in the north mining area of the mine are shown in Figure 1.

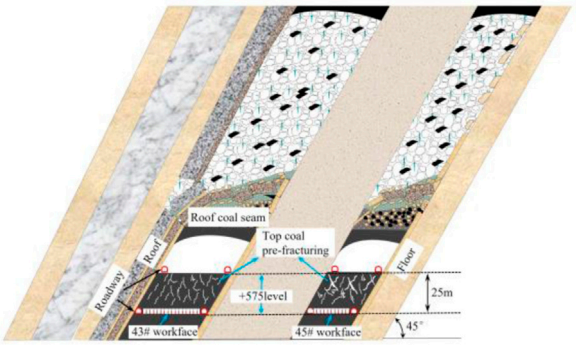

FIGURE 1
Occurrence characteristics of coal seams in the north mining area of Wudong Coal Mine.

The mine adopts the horizontal sublevel fully mechanized caving mining method. At present, the mining has been advanced to +575 level 43# and 45# seams in the north mining area. The workface has average widths of 33 m and 30.6 m, and the height of the design phase is 25 m. In the on-site mining and caving process, hard-top coal cannot be fully broken under the action of mine pressure and support disturbance, which leads to a large block size that exceeds the coal drawing port size and often causes plugging. This results in low recovery rate of the top coal, poor economic benefits, and is a serious threat to safety in production. Therefore, in the case of horizontal sublevel fully mechanized caving mining in this seam, a reasonable measurement should be adopted to pre-blast and weaken the hard-top coal so as to improve the caving ability of the top coal.

Coal sample physical and mechanical parameters test plan

Test protocol and sample preparation

The coal samples required for this test were taken from the +575 level 43# coal and 45# coal working faces in the north mining area of Wudong Coal Mine. According to the test requirements and the national standard "Method for Determination of Physical and Mechanical Properties of Coal and Rock," it is processed into Φ50 mm × 100 mm, Φ50 mm × 50 mm, and Φ 50 mm × 25 mm standard cylindrical samples. The machining accuracy is that the non-parallelism of the two ends is ≤0.05 mm, the diameter deviation of the upper and lower ends is ≤0.3 mm, and the axial deflection angle is ≤0.25°. The surface of the sample is smooth and defect-free.

To fully understand the physical and mechanical parameters, and the degradation of the steep coal sample under the effect of water, this test comprised 12 groups. Uniaxial length test, tensile test, and variational shear test on natural and water-saturated samples were carried out, and five samples were prepared for testing in each group to eliminate individual errors. The seam number rules and schemes are listed in Table 1, where 43-and 45-are samples of 43# and 45# seams, respectively. The state of the specific coal sample is treated as follows:

1) Natural state sample: Put the sample in a desiccator with water at the bottom. The bottom of the sample should be 20 mm above the water surface to maintain a certain humidity.
2) Water-saturated sample: The free soaking method was used, where the sample was put inside a container and water was added three times, with an interval of 2 h each time until the water surface was 20 mm higher than the specimen. After being soaked for 48 h, the sample was taken out of the container and the surface moisture was wiped dry. The sample was defined as a water-saturated sample and wrapped with plastic wrap for the experiment.

According to the physical parameters of the coal samples, the average densities of the 43# and 45# seams in Wudong Coal Mine are 1,315.03 kg/m^3 and 1,317.37 kg/m^3, and the average wave velocities are 1,513 m/s and 1,538 m/s, respectively. The average natural absorption rates of seams of 43# and 45# coal samples are 2.67% and 2.73%, respectively.

Test system

The uniaxial axial strength of the coal sample was determined by the SAS-2000 single triaxial rock mechanical loading system,

TABLE 1 Specimen use and size.

Usage	Number	Water-contained state	Diameter/mm	Height/mm	Quantity
Uniaxial compressive test	C43-1~5, C45-1~5	Nature	50	100	20
	C43-6~10, C45-6~10	Saturate			
Tensile strength test	T43-1~5, T45-1~5	Nature	50	25	20
	T43-6~10, T45-6~10	Saturate			
Variable angle shear test	S43-1~4, S45-1~4	Nature	50	50	20
	S43-5~10, S45-5~10	Saturate			

FIGURE 2
Test system diagram.

which can monitor the axial and radial strain at the same time. The DS5 multi-channel acoustic emission system is equipped to monitor the acoustic emission signal generated in the compression process of the coal sample in real-time, including rising count, amplitude, and energy. The sample frequency was set at 1 MHz, the acoustic emission signal detection threshold was set at 40 dB, and two AE sensors were fixed in the middle of the sample. The tensile and shear strengths were measured by using the HCT-605A tester. The test system is shown in Figure 2.

Coal sample test results and analysis

Analysis of uniaxial compression test results

In this study, uniaxial compressive tests were carried out on the coal samples with different moisture conditions taken from 43# seam and 45# seam. The detailed compressive strength and deformation parameters were obtained, and the mean values were taken for further analysis. As can be observed in the test results in Table 2, the uniaxial compressive strengths of samples of 43# and 45# seams degraded by 19.6% and 17.4%, respectively, under the influence of moisture. The elastic moduli of both samples were 15.3% under the influence of moisture.

Figure 3 shows the stress–strain curves of the experimentally obtained data. As indicated, coal samples of 43# and 45# seams of Wudong Coal Mine exhibited consistent stress–strain curves. The curves consisted of compaction stage, elastic stage, yield failure stage, and post-rupture stage. Coal samples underwent compaction and elasticity stages for a long time before failure. After reaching peak strength, the bearing capacity rapidly decreased (Zhang, et al., 2021; Liu, et al., 2022; Xue, et al., 2022).

Although stress–strain curves of natural and water-saturated coal samples showed the same trend, they were slightly different at the yield stage. The stress of natural coal samples increased continuously with the strain at the yield stage. When the stress reached the ultimate yield strength, the specimen did not fail immediately but demonstrated an abrupt reduction before growth as the strain kept increasing. During the experiment, it was observed that the sample was still able to bear the load despite the generation of the fracture, but the outer layer was broken and fell off, similar to wall caving. When subjected to continuous loading, the failure plane occurred and developed along the fracture of the specimen and continued until the end of the experiment. The water-consume-saturated coal samples had a relatively short yield stage and immediately failed upon reaching the ultimate strength, which was closely related to the existence of water. This happened because the secondary extension of fracture was blocked due to pore pressure and the incompressibility of fracture water. Finally, the specimen failed rapidly, which was accompanied by significant strength decline (Yao, et al., 2015; Lai, et al., 2021; Zhang, et al., 2021).

As shown in Figure 3, under uniaxial loading, natural coal samples mainly displayed a mixed tension–shear failure mode, where the vertical tensile fractures and certain shear fractures were significantly developed inside and the specimens were quite complete after loading. The water-saturated coal samples experienced a penetrating splitting shear failure, with an "X" shaped conjugate shear failure surface inside. The overall fracture degree of the samples was higher, and the crack propagation was more abundant.

The experimental results demonstrate that moisture-induced degradation was significant, which caused softening of the coal sample because of the reduction in the cohesion between fracture particles under the influence of water. In particular, the peak strength and elastic modulus of the samples presented a downward trend and the overall mechanical properties were weakened.

TABLE 2 Test results of compressive strength and deformation parameters of 43# and 45# coal seam in Wudong Coal Mine.

Number	Water-contained state	Average uniaxial compressive strength/MPa	Average elastic modulus/GPa	Average Poisson's ratio
C43	Nature	13.81	1.317	0.324
	Saturate	11.10	1.115	0.384
C45	Nature	13.59	1.324	0.328
	Saturate	11.22	1.122	0.383

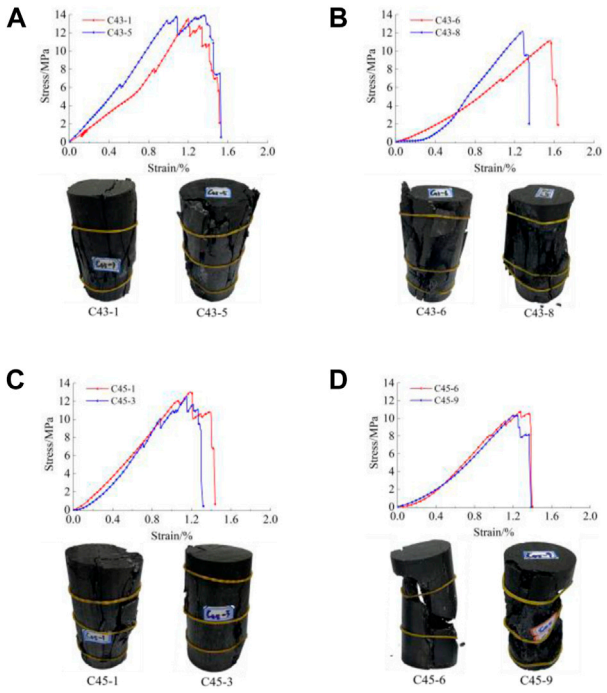

FIGURE 3
Typical uniaxial compression stress–strain curves and failure characteristics of 43# and 45# coal samples under natural and water saturation conditions. **(A)** Natural state of 43# coal samples. **(B)** Water-saturated state of 43# coal samples. **(C)** Natural state of 45# coal samples. **(D)** Water-saturated state of 45# coal samples.

Comparing the failure patterns of natural and water-saturated coal samples shows that the failure and broken blocks of water-saturated coal samples were generally more serious than those of natural samples. Therefore, in the implementation of the top-coal pre-blast scheme, water injection can soften the top coal in advance and change the crushing degree of the hard-top coal, which is of practical significance in terms of reducing the fragment size of the top coal and improving the recovery rate.

Analysis of the tensile strength test results

The results of the tensile strength test are shown in Table 3. The average tensile strengths of natural and water-saturated coal samples in 43# seam are 1.467 and 1.105 MPa, respectively. Meanwhile, the average tensile strengths of natural and water-saturated coal samples in 45# seam are 1.459 and 1.127 MPa, respectively. Moisture has a significant impact on the tensile strength of the coal samples. In particular, the tensile strengths of the coal samples obtained from 43# and 45# seams degraded by 24.68% and 22.76%, respectively, due to the softening effect of the water.

TABLE 3 Wudong Coal Mine 43#, 45# seam tensile strength test results.

Number	C43		C45	
Water-contained state	Nature	Saturate	Nature	Saturate
Average tensile strength/MPa	1.467	1.150	1.459	1.127

Figure 4 illustrates the fracturing features of the coal samples. In the Brazilian splitting experiment, an approximately vertical failure surface was generated along the primary joint of the coal sample, and the sample split into two halves along the failure surface. The main failure plane developed along the internal joints of the water-saturated coal sample, fracturing occurred locally, and the degree of fragmentation was significant.

Analysis of the shear strength test results

The shear strength test results of natural and water-saturated coal samples are shown in Table 4. According to the test results,

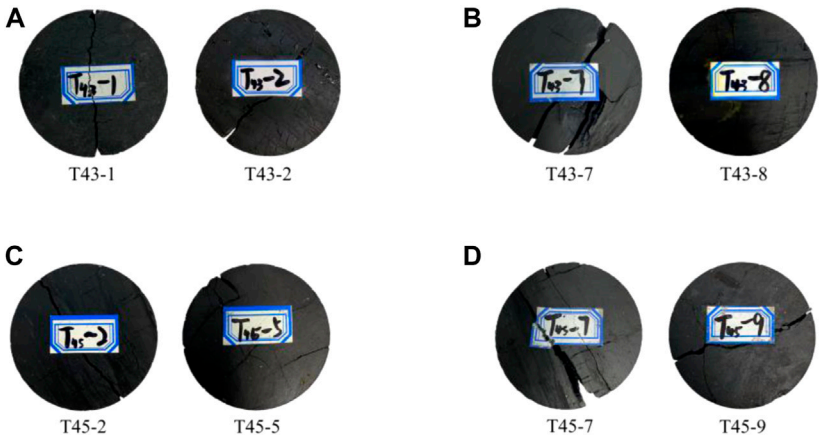

FIGURE 4
Typical coal samples splitting failure characteristics of 43# and 45# coal samples under natural and water-saturated conditions. **(A)** Natural state of 43# coal samples. **(B)** Water-saturated state of 43# coal samples. **(C)** Natural state of 45# coal samples. **(D)** Water-saturated state of 45# coal samples.

TABLE 4 Wudong Coal Mine 43#, 45# seam shear strength test results.

Number	Shear angle	P_s/ kN	σ/ MPa	τ/ MPa	Number	Shear angle	P_s/ kN	σ/ MPa	τ/ MPa
S43-1	60	5.654	1.124	1.947	S43-6	30	39.312	13.588	7.845
S43-2	60	7.044	1.412	2.446	S43-7	30	44.504	15.313	8.841
S43-3	45	21.130	5.960	5.960	S43-8	45	12.333	3.457	3.457
S43-4	45	29.779	8.332	8.332	S43-9	45	19.971	5.639	5.639
S43-5	60	3.688	6.387	6.040	S43-10	45	13.450	3.789	3.789
S45-1	45	17.813	5.026	5.026	S45-6	60	5.170	1.026	1.777
S45-2	30	63.562	21.882	12.633	S45-7	60	6.139	1.230	2.130
S45-3	30	69.569	24.257	14.005	S45-8	30	45.185	15.532	8.967
S45-4	30	65.835	22.827	13.179	S45-9	30	26.564	9.140	5.277
S45-5	60	9.511	1.921	3.328	S45-10	60	8.858	1.761	3.051

normal stress and shear stress were obtained by substituting the failure load Ps of the coal sample when it was cut into halves into Eqs 1, 2. The regression curves of normal stress and shear stress of natural and saturated coal samples under different shear angles were obtained by fitting, and Eq. 3 was used to calculate the angle of internal friction and cohesion C of coal samples (test data S43-5 and S45-9 with larger deviations were eliminated in the fitting process). The fitting results are shown in Figure 5.

$$\sigma = \frac{P_s}{A}\left(\cos\alpha + f\sin\alpha\right) \quad (1)$$

$$\tau = \frac{P_s}{A}\left(\sin\alpha - f\cos\alpha\right) \quad (2)$$

$$\tau = \sigma\tan\varphi + C \quad (3)$$

In this formula, σ is the normal stress, MPa; τ is the shear stress, MPa; P_s is the failure load of the sample, N; A is the contact area, mm^2; α is the sample placement angle, °; f is the friction coefficient of the roller, f =1/nd, n is the number of rollers; d is the diameter of the roller, mm; φ is the internal friction angle of the coal sample, °; and C is the cohesive force of the coal sample, MPa.

According to Figure 5, the shear stress along the shear plane of natural and water-saturated coal samples before failure increases with the normal stress. The cohesion of the two coal samples was 2.522 Mpa and 2.007 Mpa, respectively, and the

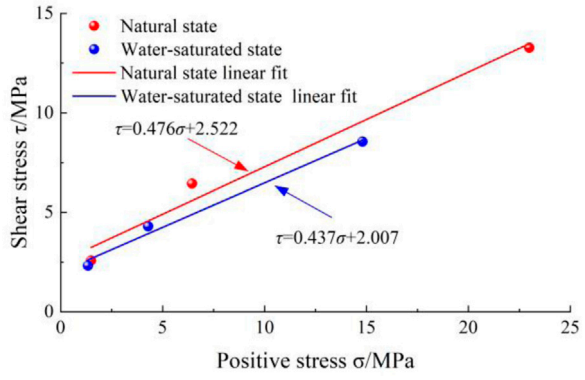

FIGURE 5
Shear strength curve of the coal samples.

degradation degree was 20.4%. The internal friction angles were 25.5° and 23.6°, respectively, and the deterioration degree was 7.5%. Hence, it could be concluded that moisture led to a severe degradation of the shear strength of the coal sample. Figure 6 shows the shear failure features of natural and water-saturated coal samples. As observed, both coal samples experienced shear failure along the shear plane, and the distributions of failure cracks on the surface were slightly different due to the different moisture conditions. The shear fractures of natural coal samples were mainly found near the shear plane, and the samples were mostly broken into halves along the shear plane, with a low degree of fragmentation. The shear surface of water-saturated coal samples sometimes deviated from the shear plane, and multiple shear fractures occurred near the shear surface, with a plentiful and high degree of fragmentation.

Analysis of acoustic emission characteristics

The acoustic emission signal was generated during the uniaxial loading on the coal sample. Based on the analysis of rising count and energy parameter, the acoustic emission evolution law and micro-failure features of the coal sample during loading were used to investigate acoustic emission features of natural and water-saturated coal samples. Specialized software was used to process acoustic emission parameters, such as rising count, accumulated rising count, and energy and accumulated energy, and the acoustic emission features of the coal sample under water–force coupling effect were analyzed (Qin, et al., 2012; Xia, et al., 2015; Zhang Y, et al., 2018). The rising count refers to the number of times that the acoustic emission signal exceeded the set detection threshold (40 dB), reflecting the number of microfractures inside the sample. Energy refers to the elastic energy released by the internal micro-fracture development of the coal sample, reflecting the degree of fragmentation. The acoustic emission and testing machine time were normalized during data processing to facilitate their synchronous analysis.

Figure 7 shows the stress, rising count, accumulated rising count, stress, energy, and accumulated energy curves under uniaxial loading of natural and water-saturated coal samples in +575 level in the north mining area in Wudong Coal Mine. As

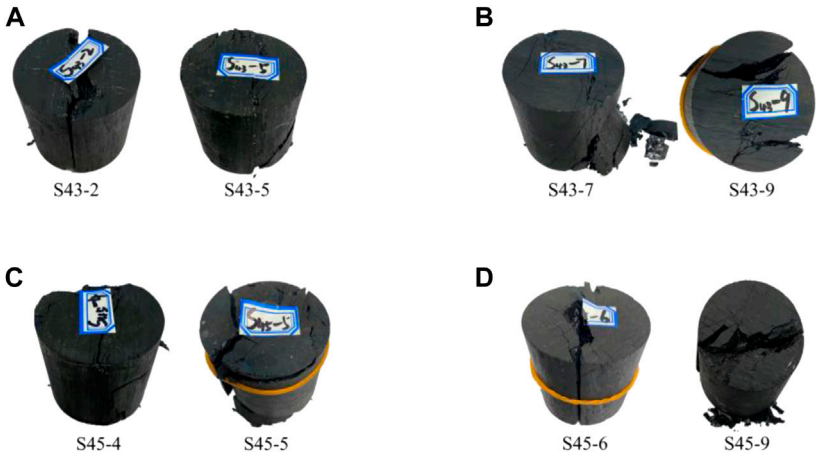

FIGURE 6
Typical coal shear failure characteristics of 43# and 45# coal samples under natural and water-saturated conditions. **(A)** Natural state of 43# coal samples. **(B)** Water-saturated state of 43# coal samples. **(C)** Natural state of 45# coal samples. **(D)** Water-saturated state of 45# coal samples.

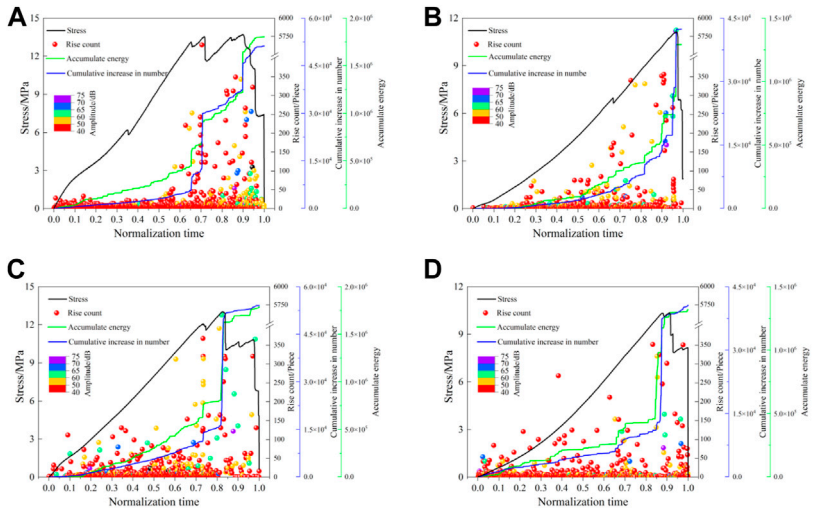

FIGURE 7
Typical coal AE characteristics of 43# and 45# coal samples under natural and water-saturated conditions. **(A)** AE characteristics in natural state of C43-5. **(B)** AE characteristics in water-saturated state of C43-6. **(C)** AE characteristics in natural state of C45-1. **(D)** AE characteristics in water-saturated state of C45-9.

observed, the acoustic emission features of natural and water-saturated samples in 43# and 45# seams did not differ much, and the acoustic emission count of each significantly increased before the peak load was achieved. Furthermore, the accumulated rising count and accumulated energy showed sharp growth, which happened because the internal fracture of the sample developed continuously and the elastic energy kept releasing at the elastic stage. Meanwhile, we found that there were differences in the details of the natural and water-saturated samples. The accumulated rising count and accumulated energy of the water-saturated samples were lower than those of natural samples. In addition, the moisture condition had a negative correlation with the acoustic emission count and energy of the coal sample (i.e., when the water content was higher, the acoustic emission count and energy became lower). This happened because the initiation and propagation of the fracture were hindered by the existence of incompressible water in fractures of the water-saturated coal samples. In addition, the absorption of the acoustic emission signal from moisture and the attenuation and disappearance of micro-elastic wave generated during the fracture development resulted in the inability to detect an acoustic emission signal due to the overly low amplitude. By statistical calculation, the low amplitude events (40–45 dB) of the natural samples obtained from 43# and 45# seams accounted for 76.43% and 72.58% of the total events, while in water-saturated samples, the percentages were 66.89% and 61.33%, respectively. This further verifies the absorption and inhibition effect of moisture on weak acoustic emission signals.

Stress distribution law of a coal body under water deterioration

In the horizontal sub-mining process of steeply inclined coal seams, the stress distribution in the top coal will change because of the collapse evolution of the roof and energy release, as well as the moisture-induced degradation. In this section, a numerical calculation model will be established, and the physical and mechanical parameters of 43# and 45# coal samples in natural and saturated state obtained from experiments will be used to investigate the stress variation laws before and after water injection. The mechanism of water injection to weaken the coal body will be further elaborated, and the top coal stress distribution features in steeply inclined coal seams after water injection will be studied to reveal the coupling characteristics of water–force coupling features in horizontal sublevel fully mechanized caving mining for the hard-top coal of steeply inclined coal seams.

3D numerical model construction and mining plan

FLAC^{3D} is widely used in the research and analysis of geotechnical and mine excavation projects because it can better simulate deformation problems such as stress, deformation, and displacement caused by excavation activity or external load disturbance. The FLAC^{3D} numerical calculation model of steep seam workface mining was established based on the geological data and the parameters of the north mining area of Wudong

TABLE 5 Physical and mechanical parameters of the main coal rocks in the northern mining area of Wudong Coal Mine.

Lithology	Bulk modulus/GPa	Shear modulus/GPa	Tensile strength/MPa	Friction angle/(°)	Cohesion/MPa	Density kg/m^3
Loess layer	0.45	0.44	0.30	22	5.42	1790
Ovulocyte layer	6.17	4.50	0.96	24	6.22	2,500
Siltstone	15.85	10.95	3.89	30	11.62	2,600
Fine sandstone	19.57	14.07	3.17	30	13.38	2,600
43# coal	**1.25**	**0.50**	**1.47**	**25.5**	**2.52**	**1,315**
43# coal full of water	**1.60**	**0.40**	**1.15**	**23.6**	**2.01**	**1,367**
45# coal	**1.28**	**0.50**	**1.46**	**25.5**	**2.52**	**1,317**
45# coal full of water	**1.60**	**0.41**	**1.13**	**23.6**	**2.01**	**1,354**
Carbonaceous peat	4.50	2.20	1.86	28	2.75	2,400
Argillaceous chalkstone	8.12	3.40	1.71	26	3.60	2,100

The bold values are the result of the previous rock mechanics tests, so they are specifically indicated for ease of distinction.

Coal Mine, which were collected by field investigation. The physical and mechanical parameters of the coal seams were obtained by a rock mechanics experiment. The specific parameters are shown in Table 5.

The mining sequence of 45# coal seam and 43# coal seam was simulated according to the historical mining sequence of the north mining area of Wudong Coal Mine. The numerical model was established until the surface with the size of 600 m × 350 m × 96 m (L × W × H), and the total of 128,020 elements and 135,681 nodes were divided. The numerical calculation model of the north mining area of Wudong Coal Mine is shown in Figure 8. The displacement boundary was applied to both sides and the bottom of the model, while displacement was free in the vertical direction. It should be noted that the stress field in the north mining area of Wudong Coal Mine plays a dominant role in horizontal tectonic stress. The maximum main stress was about 1.5–2 times larger than the gravitational stress, the gradient crustal stress of 0.025 MPa/m was applied in the vertical direction of the model, and the gradient crustal stress of 0.05 MPa/m was applied in the left-hand and right-hand directions (dip) and the front and back directions (strike), respectively.

According to the historical mining sequence, each level of steeply inclined coal seams was excavated in stages, and the survey lines were arranged along the strike in the top coal seam of 43# and 45# seams to extract the vertical stress of the top coal in the process of excavation. The top-coal stress distribution before and after water injection and mining in 43# coal seam and 45# coal seam at +575 level was analyzed.

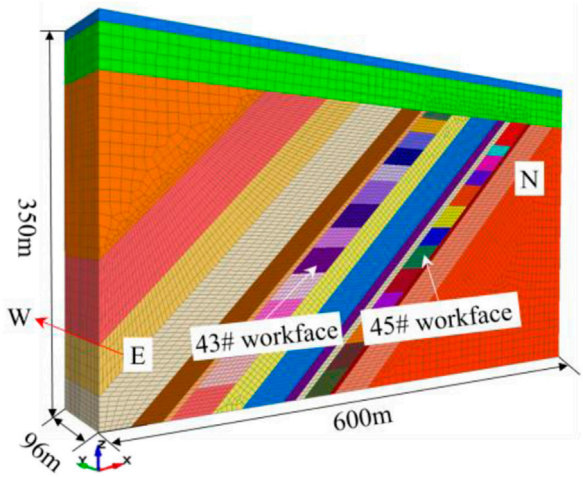

FIGURE 8
Numerical calculation model of Wudong Coal Mine North Mining Area.

Numerical calculation results and analysis

Figure 9 illustrates the vertical stress of different seams. As observed, the internal stress of 45# and 43# seams before and after water injection differed greatly: the maximum vertical stresses of 45# seam, which was located in the south upper corner, were 11.7 MPa and 7.21 MPa before and after water injection, respectively; the maximum vertical stresses of 43# seam, which was also located in the south upper corner, were 13.9 MPa and 8.47 MPa before and after water injection, respectively. This indicates that water injection caused the maximum stress to transfer downward, and the stress concentration area was significantly reduced with more uniform distribution. According to the internal stresses of the coal samples obtained from 43# and 45#, the stress of 43# seam was slightly larger than that of 45# seam. This happened because the force of the 43# coal seam roof on the 43# coal seam was larger than the force of the middle rock column on the upper left-hand of the 45# coal seam.

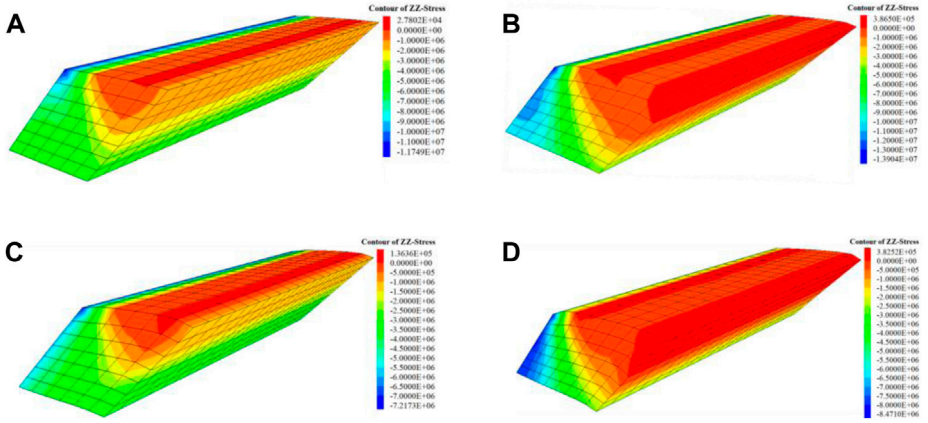

FIGURE 9
+575 level 45#, 43# coal seam stress distribution characteristics. **(A)** No water injection in 45#coal. **(B)** No water injection in 43#coal. **(C)** Water injection in 45#coal. **(D)** Water injection in 43#coal.

To quantitatively study the change of the internal stress and workface advanced support pressure of the top coal after water injection, two measuring points were arranged in the central position of the 45# and 43# seams along the advancing direction (y = 48 m and 96 m) to monitor the evolution law of the top-coal stress with the advancing degree. The measuring line was arranged in the middle of the floor of the 45# and 43# seams along the advancing direction to monitor the workface advanced support pressure. The stress evolution law of the internal measurement point of the top coal and the bottom plate of the 45# and 43# top coal is shown in Figure 10.

As observed in Figures 10A,B, the top-coal internal stress was significantly reduced after water injection. This indicates that top coal was fully weakened. As the advance continued, the vertical stress of each monitoring site presented an increasing trend, except for the advance at 28.8–38.4 m and 76.8–86.4 m with reduced stress. This happened because under this advancement, the monitoring sites had already reached within the reduction zone of advanced support pressure. Additionally, the top-coal stress of 43# seam was lower than that of 45# seam. This happened because 45# coal seam was first mined at the +575 level, and the mining in 45# coal seam played a similar role as mining in the protective layer in 43# coal seam, which effectively released the top-coal stress of 43# seam. Therefore, it not only improved the release rate of top coal but also reduced the outburst risk of the seam.

Figures 10C,D shows the evolution laws of floor advanced support pressures of 45# and 43# workfaces. As observed, water injection not only had a great impact on floor advanced support pressure, but it also weakened the peak pressure. Specifically, the peak advanced support pressure of 45# seam after water injection was 50%–65% of that before water injection, while the advanced peak support pressure of 43# seam after water injection was 63%–72% of that before water injection. This further demonstrates the significant weakening effect of water.

Engineering design

According to the occurrence characteristics and actual production conditions of the steeply inclined coal seams of the fully mechanized caving face in the north mining area of Wudong Coal Mine, as well as the aforementioned results, this study found that when implementing the pre-blast scheme for the top coal of the +575 level coal workface in the north mining area of Wudong Coal Mine, the top-coal water-injection weakening measure can be used in advance to improve the crushing degree of the top coal and increase the caving. Therefore, it was designed to implement top-coal water-injection weakening measures 30 m ahead of the north roadway of the 45# coal seam working face at +575 level. The same drill hole was used for water injection and blasting, and high-pressure water was used to fracture the seam. The length of the sealing hole of the water-injection hole was 10 m, and the diameter of the hole was Φ113 mm. The range of water-injection pressure and the amount of water injected are given by the following calculation (Kang, et al., 2004; Zhang Q, et al., 2018; Wang, et al., 2020):

$$P_D = (0.4 - 0.5)H \tag{4}$$

$$P_0 = 156 - \frac{88}{(0.001H + 0.8)} \tag{5}$$

$$T = l \cdot a \cdot h \cdot \gamma \tag{6}$$

$$M_K = K \cdot T \cdot W \tag{7}$$

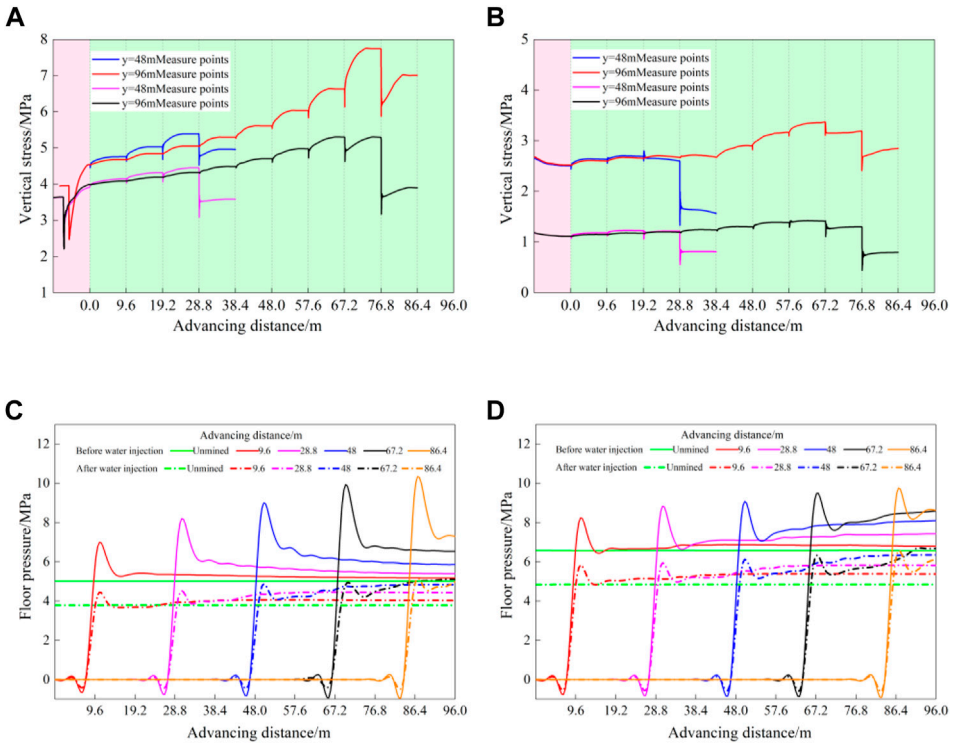

FIGURE 10
Stress evolution law of the internal measurement point of the 45# and 43# top coal and the floor. **(A)** Stress evolution law of 45# top coal. **(B)** Stress evolution law of 43# top coal. **(C)** Stress evolution law of 45# floor. **(D)** Stress evolution law of 43# floor.

In the formula, P_D is the formation pressure of the coal seam, kg/m^2; H is the burial depth of the coal seam, m; P_0 is the minimum pressure of water injection in the coal seam, MPa; l is water-injection length, m, take 20; a is borehole spacing, m, take 5; h is coal seam thickness, m, take 22; γ is coal density, t/m^3, take 1.316; M_K is the water injection amount of a single hole, t; T is the amount of wet coal borne by the borehole, t; W is the water absorption rate of the coal seam, %, to be taken as 2.7; and K is the coefficient of water imbalance, to be taken as 0.5 to 1.0.

The burial depth of the +575 level in the north mining area of Wudong Coal Mine is 260 m. The reference range of coal seam water-injection pressure is obtained by putting H=260 m into Eqs 4, 5 . The calculation results are P_D =10.4–11.7 MPa, P_0 =5.4 Mpa. According to the actual water injection situation of the 45# coal seam working face, the water-injection pressure of the coal seam is determined to be 10 Mpa. According to Eqs 6, 7, the water-injection volume is 39.09 tons.

Conclusion

1) Water-softening had a significant effect on the mechanical properties of the coal samples. Owing to the effect of water-softening, the deterioration degrees of uniaxial compressive strength of 43# and 45# coal seam coal samples were 19.6% and 17.4%, respectively, the deterioration degrees of elastic modulus were both 15.3%, and the deterioration degrees of tensile strength were 24.68% and 22.76%, respectively. In addition, the deterioration degree of cohesion was 20.4%, and the deterioration degree of internal friction angle was 7.5%.
2) The failure and the degree of broken pieces of water-saturated samples were generally more severe than those of natural samples. Moisture-induced degradation was obvious—the cohesion between fracture particles was destroyed due to water, causing the softening of the coal sample and worsening the overall mechanical properties.
3) Moisture condition was negatively correlated with acoustic emission count and energy. The accumulated rising count and accumulated energy of water-saturated samples were

lower than those of natural samples. This happened because of the existence of incompressible water in the fractures of the water-saturated coal samples, which hindered the initiation and propagation of fractures. Water exerted a repression effect on the absorption of weak acoustic emission signals, and part of the small elastic waves generated by fracture development attenuated and disappeared in the fracture water.

4) Numerical simulation studies showed that the internal stress of 45# and 43# coal bodies before and after water injection was evidently different. The water injection had a significant impact on the internal stress of the top coal and the advanced support pressure of the working surface base, which fully weakened the coal body. The stress in the coal body was released and transferred after water injection, the pressure peak was weakened, and the internal stress of the top coal and the advanced support pressure of the bottom plate was evidently reduced.
5) For the field project, we produced a specific water-injection weakening design. The design parameters are as follows: it was arranged 30 m ahead of the north lane of the working face; the length of the sealing hole of the water-injection hole was 10 m, the diameter of the hole was Φ113 mm, the water-injection pressure was 10 Mpa, and the water-injection volume per hole was 39.09 tons. By injecting water into the top coal of the working surface in advance to weaken it, the degree of crushing of the hard-top coal was changed, which was a significant development for the safe and efficient production of this steeply inclined working surface.

Data availability statement

The original contributions presented in the study are included in the article/Supplementary Material; further inquiries can be directed to the corresponding author.

Author contributions

LZ and XL conceived the research. LZ analyzed the data and wrote the manuscript. RB participated in the design of the study and verified the results. All authors have read and approved the final manuscript.

Funding

This research was funded by the National Natural Science Foundation of China (No. 52004201), Shaanxi Provincial Natural Science Basic Research Project Enterprise Joint Fund (No. 2019JLZ-04), and the Natural Science Foundation of Shaanxi Provincial Department of Education (No. 20JK0765).

Acknowledgments

We thank the National Natural Science Foundation of China (No. 52004201), Shaanxi Provincial Natural Science Basic Research Project Enterprise Joint Fund (No. 2019JLZ-04), and the Natural Science Foundation of Shaanxi Provincial Department of Education (No. 20JK0765) for its support of this study. We thank the academic editors and reviewers for their kind suggestions and valuable comments.

Conflict of interest

RB was employed by the National Energy Group Ningxia Coal Industry Co., Ltd. Qingshuiying Coal Mine.

The remaining authors declare that the research was conducted in the absence of any commercial or financial relationships that could be construed as a potential conflict of interest.

Publisher's note

References

Cui, F., Lai, X. P., Cao, J. T., and Shan, P. F. (2015). Strength deterioration study of coal and rock mass affected by coupled-crack. *Chin. J. Rock Mech. Eng.* 34 (2), 3633–3641. doi:10.13722/j.cnki.jrme.2014.0564

Dai, H. Y., Yi, S. H., Ju, W. J., Yan, Y. G., Yang, S. J., and Qiao, Z. D. (2006). Law of strata and surface movement due to horizontally-sliced mechanized top-caving mining at steep-inclined super-thick coal seam. *J. Univ. Sci. Technol. Beijing* 28 (5), 409–412. doi:10.13374/j.issn1001-053x.2006.05.022

Deng, G. Z., Wang, S. B., and Huang, B. X. (2004). Study on the behaviour of hydraulic crack propagation in coal and rock. *Chin. J. Rock Mech. Eng.* 23 (20), 3489–3493. doi:10.3321/j.issn:1000-6915.2004.20.018

Ju, W. J., Li, Q., Wei, D., and Dai, H. Y. (2006). Pressure character in caving steep-inclined and extremely thick coal seam with horizontally grouped top-coal drawing mining method. *J. China Coal Soc.* 31 (5), 558–561. doi:10.3321/j.issn:0253-9993.2006.05.002

Kang, T. H., Zhang, J. P., and Bai, S. W. (2004). Theoretical study and application of weakening top coal using water pre-infusion in fully mechanized sublevel caving mining. *Chin. J. Rock Mech. Eng.* 23 (15), 2615–2621. doi:10.3321/j.issn:1000-6915.2004.15.025

Lai, X. P., Bai, R., Cao, J. T., Shan, P. F., Fang, P. F., Fang, X. W., et al. (2021). Experimental study on mechanical and acoustic characteristics of interbedded rock specimens under cyclic loading. *J. Xi' Univ. Sci. Technol.* 41 (6), 955–963. doi:10.13800/j.cnki.xakjdxxb.2021.0601

Lai, X. P., Dai, J. J., and Li, C. (2020). Analysis on hazard characteristics of overburden structure in steeply inclined coal seam. *J. China Coal Soc.* 45 (1), 122–130. doi:10.13225/j.cnki.jccs.YG19.1405

Lai, X. P., Wang, N. B., Xu, H. D., Qi, T., Cao, J. T., and Jiang, D. H. (2009). Safety top-coal-caving of heavy and steep coal seams under complex environment. *J. Univ. Sci. Technol. Beijing* 31 (3), 277–280. doi:10.13374/j.issn1001-053x.2009.03.030

Lai, X. P., Zhang, L. M., Zhang, Y., Shan, P. F., Wan, P. F., and Mu, K. W. (2022). Research of the backfill body compaction ratio based on upward backfill safety mining of the close-distance coal seam group. *Geofluids* 2022, 1–11. Article ID 8418218. doi:10.1155/2022/8418218

Li, M. Z. (2018). *Research on key technology of fully mechanized caving mining with large mining height in hard and extra thick coal seam in Yushen mining area*. [Beijing: General Research Institute of Coal Science. [dissertation/master's thesis].

Liu, J., Xue, Y., Zhang, Q., Wang, H. M., and Wang, S. H. (2022). Coupled thermo-hydro-mechanical modelling for geothermal doublet system with 3D fractal fracture. *Appl. Therm. Eng.* 200, 117716. doi:10.1016/j.applthermaleng.2021.117716

Qian, M. G., Xu, J. L., and Wang, J. C. (2018). Further on the sustainable mining of coal. *J. China Coal Soc.* 43 (1), 1–13. doi:10.13225/j.cnki.jccs.2017.4400

Qin, H., Huang, G., and Wang, W. Z. (2012). Experimental study of acoustic emission characteristics of coal samples with different moisture contents in process of compression deformation and failure. *Chin. J. Rock Mech. Eng.* 31 (6), 1115–1120. doi:10.3969/j.issn.1000-6915.2012.06.004

Shi, P. W., and Gao, Z. N. (2003). The failure laws of surrounding rocks and overlying bed in the stereo special thickness seam mining. *J. China Coal Soc.* 28 (1), 13–16. doi:10.3321/j.issn:0253-9993.2003.01.003

Suo, Y. L. (2001). Study of pre-weakened method on the hard thick-top-coal in fully mechanized caving. *J. China Coal Soc.* 26 (6), 616–620. doi:10.3321/j.issn:0253-9993.2001.06.011

Wang, G., Fan, J. Y., Wang, W. R., and Xu, H. (2020). Research on slot spacing model for hydraulic slot-assisted directional fracturing of coal mass. *J. Min. Saf. Eng.* 37 (3), 622–631. doi:10.13545/j.cnki.jmse.2020.03.022

Wang, J. C., Bai, X. J., Wu, Z. S., and Xiong, D. H. (2000). Research on the fractured blocks of the top-coal in the longwall top-coal caving technique of the hard coal seam. *J. China Coal Soc.* 25 (3), 238–242. doi:10.13225/j.cnki.jccs.2000.03.005

Wang, J. C. (2018). Engineering practice and theoretical progress of top coal mining in China. *J. China Coal Soc.* 43 (1), 43–51. doi:10.13225/j.cnki.jccs.2017.4101

Wu, S. Q., and Shi, P. W. (1990). The study of rock pressure manifestation in steep seam. *J. Xi' Min. Inst.* 10 (2), 1–9. doi:10.13800/j.cnki.xakjdxxb.1990.02.001

Wu, Y. P., Yun, D. F., Xie, P. S., Wang, H. W., Lang, D., and Hu, B. S. (2020). Progress, practice and scientific issues in steeply dipping coal seams fully-mechanized mining. *J. China Coal Soc.* 45 (1), 24–34. doi:10.13225/j.cnki.jccs.YG19.0494

Xia, D., Yang, T. H., Xu, Tao., Wang, P. T., and Zhao, Y. C. (2015). Experimental study on AE properties during the damage process of water-saturated rock specimens based on time effect. *J. China Coal Soc.* 40 (S2), 337–345. doi:10.13225/j.cnki.jccs.2015.0440

Xie, H. P., Wang, J. C., Chen, Z. H., Xie, J. Q., Yan, Z. Y., and Tian, L. J. (1999). Study on top-coal blasting technique of full-mechanized caving in the hard thick coal seam. *J. China Coal Soc.* 24 (4), 16–20. doi:10.1088/0256-307X/15/12/024

Xue, Y., Liu, J., Ranjith, P. G., Gao, F., Xie, H. P., and Wang, J. (2022). Changes in microstructure and mechanical properties of low-permeability coal induced by pulsating nitrogen fatigue fracturing tests. *Rock Mech. Rock Eng.* doi:10.1007/s00603-022-03031-2

Yang, Z. W. (2014). *Research on combined weakened top coal technology of "water injection-blasting" in fully mechanized caving mining in Yungang Mine*. [dissertation/master's thesis]. Fuxin, China: Liaoning University of Engineering and Technology.

Yao, Q. L., Li, X. H., Zhou, J., Ju, M. H., Chong, Z. H., and Zhao, B. (2015). Experimental study of strength characteristics of coal specimens after water intrusion. *Arab. J. Geosci.* 8 (9), 6779–6789. doi:10.1007/s12517-014-1764-5

Zhang, Q., Ge, C. G., Li, W., Jiang, Z. B., Chen, J. X., and Li, B. G. (2018). A new model and application of coalbed methane high efficiency production from broken soft and low permeable coal seam by roof strata-in horizontal well and staged hydraulic fracture. *J. China Coal Soc.* 43 (1), 150–159. doi:10.13225/j.cnki.jccs.2017.1422

Zhang, Y., and Cao, S. G. (2021). Control of water-flowing fracture development with solid backfill mining: Designing a backfill body compression ratio for water resources protection. *Mine Water Environ.* 40 (4), 877–890. doi:10.1007/s10230-021-00821-y

Zhang, Y., Cao, S. G., Guo, S., Wan, T., and Wang, J. J. (2018). Mechanisms of the development of water conducting fracture zone in overlying strata during short wall block backfill mining: A case study in northwestern China. *Environ. Earth Sci.* 77 (14), 543. doi:10.1007/s12665-018-7726-6

Zhang, Y., Cao, S. G., Zhang, N., and Zhao, C. Z. (2020). The application of short-wall block backfill mining to preserve surface water resources in Northwest China. *J. Clean. Prod.* 261, 121232. doi:10.1016/j.jclepro.2020.121232

Zhang, Y., Liu, Y. Z., Lai, X. P., and Gao, J. M. (2021). Physical modeling of the controlled water-flowing fracture development during short-wall block backfill mining. *Lithosphere* 2021, 13. Article ID 2860087. doi:10.2113/2021/2860087